Computers and Structures 131 (2014) 56–69

Contents lists available at ScienceDirect

Computers and Structures

journal homepage: www.elsevier.com/locate/compstruc

# Modeling the warping displacements for discontinuously varying arbitrary cross-section beams

Kyungho Yoon, Phill-Seung Lee *

*Department of Ocean Systems Engineering, Korea Advanced Institute of Science and Technology, 291 Daehak-ro, Yuseong-gu, Daejeon 305-701, Republic of Korea*

ARTICLE INFO

*Article history:*
Received 20 June 2013
Accepted 24 October 2013
Available online 14 November 2013

*Keywords:*
Beams
Torsion
Twisting
Warping
Finite elements
Varying cross-section

ABSTRACT

In this paper, we propose a new and efficient warping displacement model to ensure the continuity of warping in beams with discontinuously varying arbitrary cross-sections. We briefly review the formulation of the continuum mechanics based beam finite elements allowing warping displacements. We then propose three basis warping functions: one free warping function and two interface warping functions. The entire warping displacement field is constructed by a combination of the three basis warping functions with warping degrees of freedom (DOFs). We also propose a new method to simultaneously calculate the free warping function and the corresponding twisting center. Based on this method, the interface warping functions and the twisting centers at the interface cross-sections are obtained by solving a set of coupled equations at the interface of two different cross-sections. Several beam problems with discontinuously varying cross-sections are numerically solved. The effectiveness of the proposed model is demonstrated by comparing the numerical results with those obtained by refined solid and shell finite element models.



## 1. Introduction

Beams widely used in many engineering applications have been analyzed by the finite element method. It is well known that appropriate consideration of the warping effect in the finite element analysis of beams is crucial for an accurate prediction of their twisting behavior [1–3].

Numerous studies on the warping effect have been done for many years [4–17]. When a non-constrained prismatic beam is subjected to uniform torsional moment, its cross-sections undergo constant warping deformation and the free warping behavior can be analyzed by St. Venant torsion theory [4–6]. In thin-walled cross-section beams, more general non-uniform torsion cases and constrained warping deformations can be considered by Vlasov's thin-walled beam theory [7,8]. Additionally, there have been studies on shear warping effects [9–16] and secondary warping effects [16,17].

In displacement-based beam finite element formulations, warping effects can be accounted for by adding warping displacement fields to Timoshenko's basic displacement fields. It is very important to appropriately construct the additional warping displacement fields in the beam formulations and there have been many studies, see Refs. [18–24] and therein. Most previous studies have focused on relatively simple continuously varying cross-section beams, such as prismatic and tapered beams, see Fig. 1(a). When the cross-section discontinuously varies along the beam length as shown in Fig. 1(b), the variation in the warping displacement is very complicated. Most existing formulations cannot properly represent the complicated warping behavior.

To describe the torsional warping effect in discontinuously varying thin-walled cross-section beams, a kinematic compatibility condition has been proposed to consider the interaction between two different cross-sections at a discontinuous interface [8,11]. The warping displacement models require a single warping DOF at each beam node in thin-walled cross-section beams. When a discontinuously varying cross-section beam is subjected to torsion, the twisting center also varies along the beam length. However, this effect is not considered in the previous beam formulations.

An easy and simple method of modeling the warping displacements in discontinuously varying cross-section beams is to discretize the beam cross-sections with cross-sectional elements and nodes and to properly construct the continuity of nodal warping DOFs between two cross-sectional meshes at the interface [25–28]. Since, in this warping displacement model, a large number of warping DOFs is required at each beam node and the number of warping DOFs depends on the cross-sectional meshes used, this warping displacement model has not been widely used.

In this study, we develop a new and efficient modeling method to construct the continuous warping displacement fields for discontinuously varying arbitrary cross-section beams. In order to model the continuity of warping, we define three basis warping

* Corresponding author.
*E-mail address:* phillseung@kaist.edu (P.S. Lee).

0045-7949/$ - see front matter 
http://dx.doi.org/10.1016/j.compstruc.2013.10.013

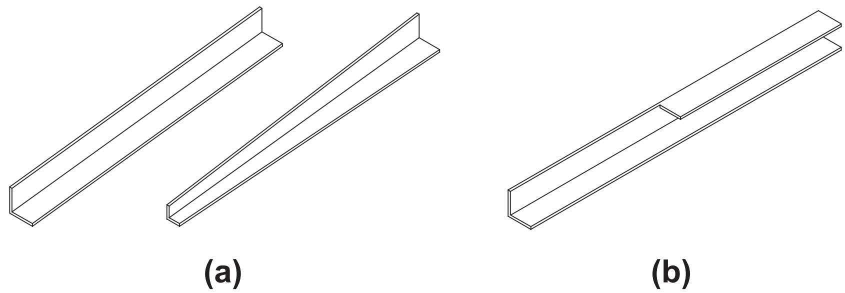


**Fig. 1.** Various beam problems. (a) Beam problems with continuous varying cross-section (prismatic and tapered beams), (b) Beam problem with discontinuously varying cross-section.

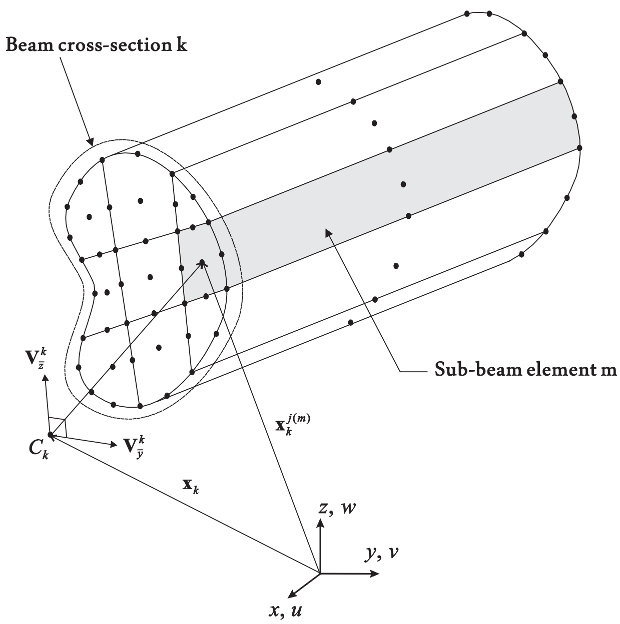


**Fig. 2.** A continuum mechanics based beam finite element assembled with nine sub-beam elements.

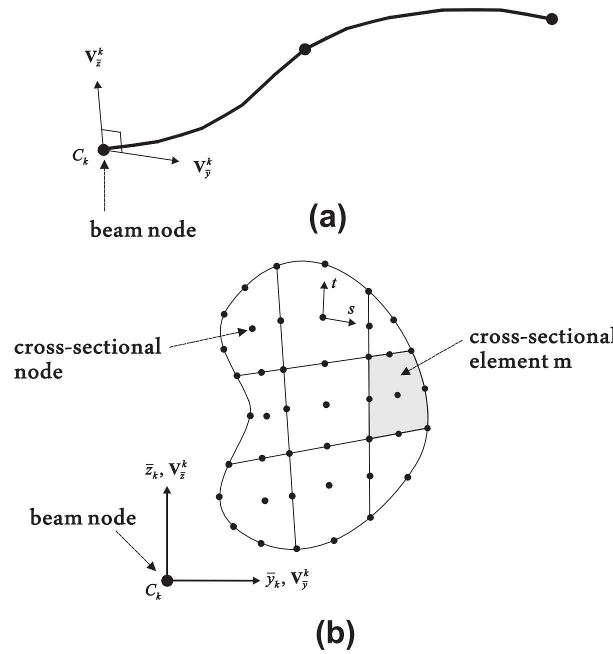


**Fig. 3.** A continuum mechanics beam finite element with cross-sectional mesh. (a) 3-Node beam finite element, (b) cross-sectional mesh at beam node *k*.

functions (one free warping function and two interface warping functions) and the corresponding warping DOFs. The basis warping functions are multiplied by the corresponding warping DOFs and interpolated along the beam length. Therefore, in our warping displacement model, at most three warping DOFs are required at each beam node for torsional warping displacement fields. Furthermore, the three warping DOFs can be condensed when the same functions exist among the basis warping functions.

The obtained warping displacement fields are not only continuous in the entire domain of the beams, but also fully coupled with the other basic behaviors of the beam (stretching, shearing, and bending) by employing the formulation of continuum mechanics based beam finite elements as proposed in our previous study [24]. The greatest advantage of the continuum mechanics based beam finite elements is their modeling ability to easily deal with very complicated beam geometries. In the warping displacement model, it is crucial to obtain the correct twisting centers. Otherwise, the warping effect coupled with stretching, shearing, and bending cannot be properly considered and erroneous responses will be obtained.

The most challenging issue in this study is how to calculate the interface warping functions without knowing the twisting centers at the interfaces. In order to solve this problem, we develop a new method to simultaneously calculate the free warping function and the corresponding twisting center. Based on the method, the interface warping functions and the corresponding twisting center are also simultaneously calculated by solving a set of coupled equations at interfaces where the cross-section discontinuously varies. In the coupled equations, the Lagrange multiplier is employed to enforce the continuity of warping at the interface.

In the following sections, we first briefly review the formulation of the continuum mechanics based beam finite elements. We then propose how to construct the continuous warping displacement fields with the three basis warping functions and a numerical method to obtain the basis warping functions. We present four numerical examples: a step varying solid cross-section problem, a discontinuously varying thin-walled cross-section problem, a partially constrained cross-section problem, and a curved beam problem with a discontinuously varying cross-section. The results are compared with reference solutions obtained by refined solid and shell element models. Finally, conclusions are given.

## 2. Modeling of warping displacement fields

In this section, based on the formulation of the continuum mechanics based beam finite element allowing warping

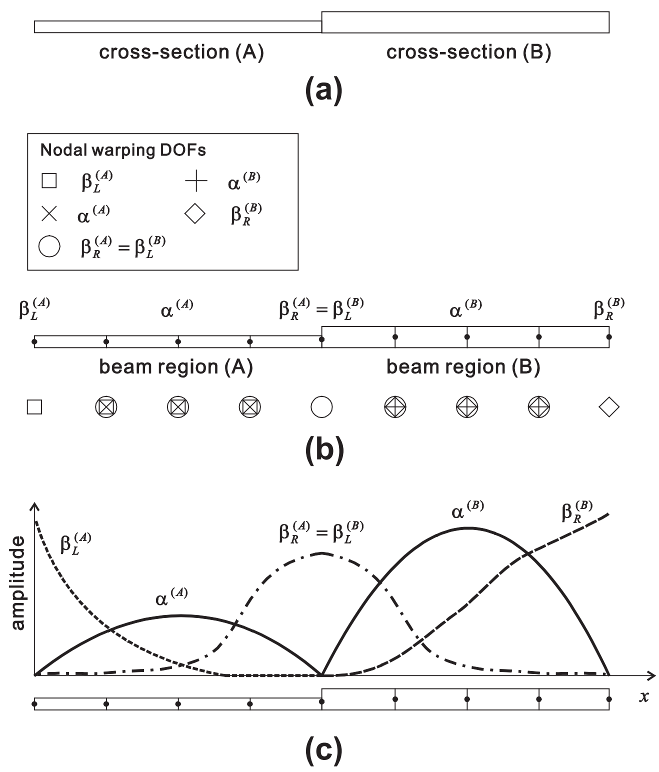


**Fig. 4.** Warping DOFs used for a discontinuously varying cross-section beam. (a) A discontinuously varying cross-section beam, (b) finite element model and warping DOF used at each nodes, (c) individual amplitude of the basis warping functions along the beam length.

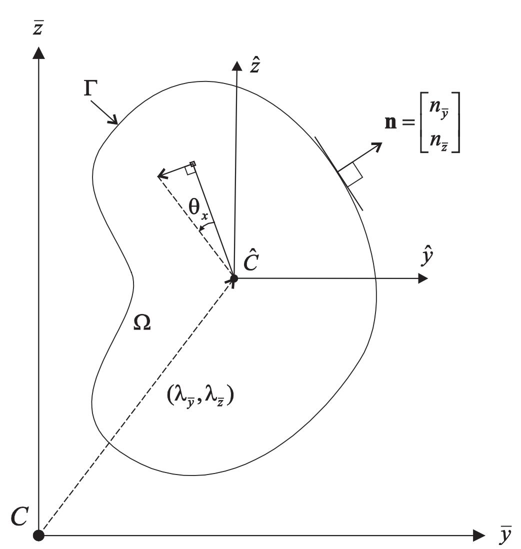

**Fig. 5.** Twisting kinematics and twisting center.

displacements [24], we introduce a new approach to constructing the continuity of warping with the definition of three basis warping functions. In the beam formulation, warping is fully coupled with bending, shearing, and stretching. The beam element can consider free/constrained warping conditions and uniform/non-uniform torsions, and model eccentricities, curved geometries, continuously varying cross-sections, as well as arbitrary cross-sections (including thin/thick-walled, open/closed, and single/multi-cell cross-sections) [24].

### 2.1. Continuum mechanics based beam finite elements

The formulation of continuum mechanics based beam finite elements is directly derived from an assemblage of $n$ solid finite elements. As shown in Fig. 2, a beam can be modeled by 3-D solid elements and the geometry interpolation of the $l$-node solid element $m$ is given by

$$\mathbf{x}^{(m)} = \sum_{i=1}^{l} h_i(r,s,t)\mathbf{x}_i^{(m)} \tag{1}$$

in which $\mathbf{x}^{(m)}$ is the material position vector, $h_i(r,s,t)$ denotes the 3-D shape function for the usual isoparametric procedure, and $\mathbf{x}_i^{(m)}$ is the $i$th nodal position vector.

When the nodes are positioned in the beam cross-sections, the 3-D shape function in Eq. (1) can be replaced by the multiplication of 1-D and 2-D shape functions

$$\mathbf{x}^{(m)} = \sum_{k=1}^{q} h_k(r)\sum_{j=1}^{p} h_j(s,t)\mathbf{x}_k^{j(m)}, \tag{2}$$

where $q$ is the number of the beam cross-sections, $p$ is the number of nodes of the solid element $m$ positioned at each beam cross-section, $h_k(r)$ and $h_j(s,t)$ are the 1-D and 2-D shape functions, respectively, and $\mathbf{x}_k^{j(m)}$ is the $j$th nodal position vector of the solid element $m$ in the beam cross-section $k$. This degeneration procedure is graphically represented in Figs. 2 and 3.

The kinematic assumption of Timoshenko beam theory is applied by

$$\mathbf{x}_k^{j(m)} = \mathbf{x}_k + \bar{y}_k^{j(m)}\mathbf{V}_{\bar{y}}^k + \bar{z}_k^{j(m)}\mathbf{V}_{\bar{z}}^k, \tag{3}$$

where the unit vectors $\mathbf{V}_{\bar{y}}^k$ and $\mathbf{V}_{\bar{z}}^k$ are the directors placed in the beam cross-section $k$, the two vectors and the position $\mathbf{x}_k$ at the beam node $C_k$ define the $k$ th cross-sectional Cartesian coordinate system, as shown in Figs. 2 and 3. The coordinates $\bar{y}_k^{j(m)}$ and $\bar{z}_k^{j(m)}$ represent the position of the $j$th cross-sectional node in the cross-sectional Cartesian coordinate system. Note that, while the cross-sectional nodes are positioned in the cross-sections to define the cross-sectional geometry, the beam nodes are positioned along the longitudinal axis given by $\mathbf{x}_k$, see Fig. 3.

Using Eq. (3) in Eq. (2), the geometry interpolation of the continuum mechanics based beam finite element corresponding to the solid element $m$ is obtained as

$$\mathbf{x}^{(m)} = \sum_{k=1}^{q} h_k(r)\mathbf{x}_k + \sum_{k=1}^{q} h_k(r)\bar{y}_k^{(m)}\mathbf{V}_{\bar{y}}^k + \sum_{k=1}^{q} h_k(r)\bar{z}_k^{(m)}\mathbf{V}_{\bar{z}}^k \tag{4}$$

$$\text{with} \quad \bar{y}_k^{(m)} = \sum_{j=1}^{p} h_j(s,t)\bar{y}_k^{j(m)}, \quad \bar{z}_k^{(m)} = \sum_{j=1}^{p} h_j(s,t)\bar{z}_k^{j(m)}, \tag{5}$$

where $\bar{y}_k^{(m)}$ and $\bar{z}_k^{(m)}$ denote the material position in the beam cross-section. Then, Eq. (4) becomes the geometry interpolation of the sub-beam $m$ corresponding to the solid element $m$. The continuum mechanics based beam finite element consists of $n$ sub-beams. Note that Eq. (5) becomes the geometry interpolation of the cross-sectional element $m$ in the cross-sectional mesh shown in Fig. 3(b).

The displacement interpolation of the sub-beam $m$ is derived from Eq. (4) as for general curved beam finite elements in Ref. [1]

$$\mathbf{u}^{(m)} = \sum_{k=1}^{q} h_k(r)\mathbf{u}_k + \sum_{k=1}^{q} h_k(r)\bar{y}_k^{(m)}\{\boldsymbol{\theta}_k \times \mathbf{V}_{\bar{y}}^k\} + \sum_{k=1}^{q} h_k(r)\bar{z}_k^{(m)}\{\boldsymbol{\theta}_k \times \mathbf{V}_{\bar{z}}^k\} \tag{6}$$

$$\text{with} \quad \mathbf{u}_k = \begin{bmatrix} u_k \\ v_k \\ w_k \end{bmatrix} \quad \text{and} \quad \boldsymbol{\theta}_k = \begin{bmatrix} \theta_x^k \\ \theta_y^k \\ \theta_z^k \end{bmatrix}. \tag{7}$$

The basic displacement field in Eq. (6) consists of Timoshenko's six deformation modes: one stretching, two transverse shearing, one

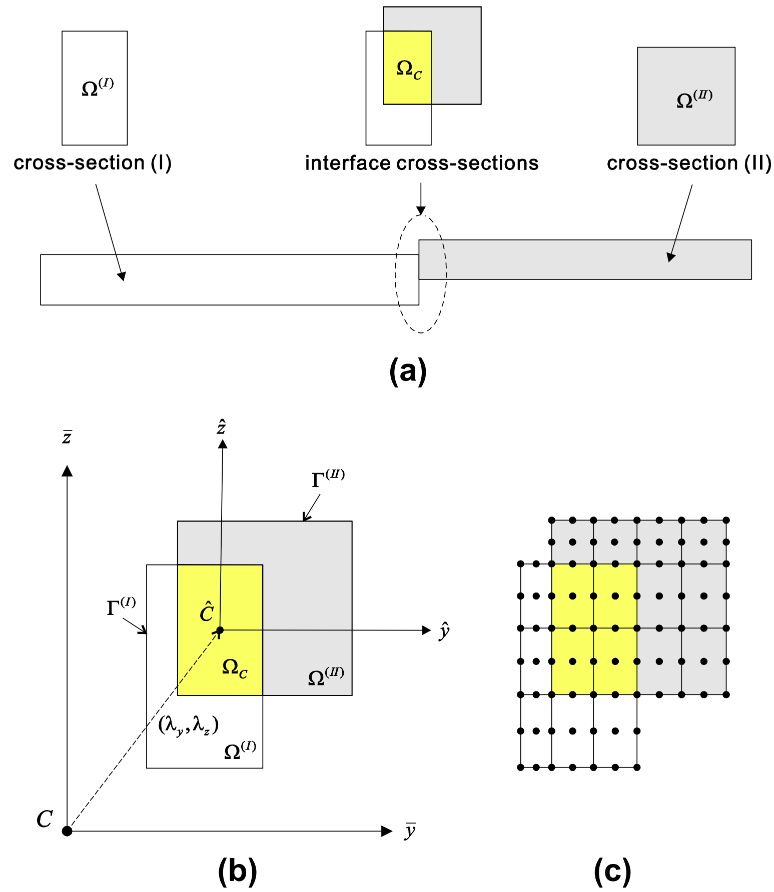


**Fig. 6.** Cross-sections of a discontinuously varying cross-section beam. (a) Cross-sections (I) and (II), and their interface $\Omega_C$, (b) interconnected domain and twisting center, (c) cross-sectional meshes used at the interface.

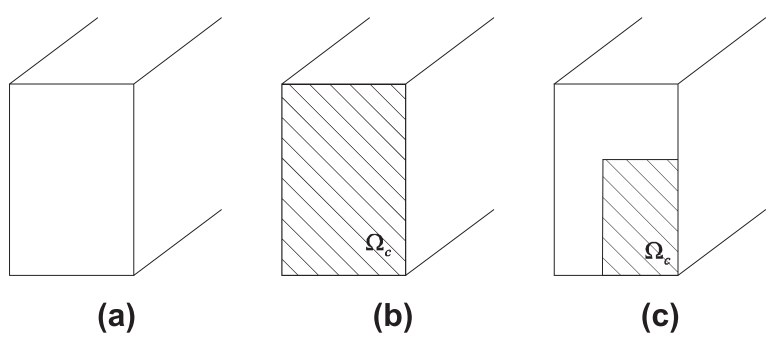


**Fig. 7.** Three special cases for the interface warping functions. (a) Free interface, (b) fully constrained interface, (c) partially constrained interface.

twisting and two bending modes. To include the warping mode, the new warping displacements $\mathbf{u}_w^{(m)}$ should be added to Eq. (6). Then, the generalized displacement field allowing warping displacements is obtained

$$\mathbf{u}_g^{(m)} = \mathbf{u}^{(m)} + \mathbf{u}_w^{(m)}. \tag{8}$$

Similarly, we can include other deformation modes as well, including shear warping modes, secondary warping modes, cross-sectional distortion modes and so on.

Based on the cross-sectional discretization at beam node $k$ in Fig. 3, two modeling methods can be employed to construct the continuous warping displacements. The first model uses

$$\mathbf{u}_w^{(m)} = \sum_{k=1}^{q} h_k(r) \sum_{j=1}^{p} h_j(s,t) f_k^{j(m)} \mathbf{V}_r^k, \tag{9}$$

where $f_k^{j(m)}$ are warping DOFs at each cross-sectional node and $\mathbf{V}_r^k$ is the director vector normal to the cross-sectional plane $k$. In this model, the total number of degrees of freedom for warping at each beam node is the same as the number of cross-sectional nodes in each cross-sectional plane. Non-uniform torsion and constraint warping cases can be easily handled as well as uniform torsion and free warping cases. As mentioned in Introduction, this method can be used for both discontinuously and continuously varying beams, but too many warping DOFs are required depending on the cross-sectional meshes used.

In the second model, the free warping function and the corresponding warping DOF are used to construct the warping displacement field

$$\mathbf{u}_w^{(m)} = \sum_{k=1}^{q} h_k(r) f_k^{(m)}(s,t)\alpha_k \mathbf{V}_r^k \quad \text{with} \quad f_k^{(m)}(s,t) = \sum_{j=1}^{p} h_j(s,t) f_k^{j(m)} \tag{10}$$

in which $f_k^{(m)}(s,t)$ is the free warping function and $\alpha_k$ is the warping DOF at beam node $k$. In Eq. (10), $f_k^{j(m)}$ is the pre-calculated free warping values at cross-sectional nodes by solving St. Venant equations in the cross-sectional plane $k$. Then, only one DOF is used for continuous warping displacements at each beam node. Note that the free warping function is used as a basis function and the entire warping displacement field has the interpolation along the beam length direction by using the warping DOFs. Therefore, the warping displacement can consider uniform/non-uniform torsion, and free and constraint warping cases. However, this interpolation method is valid only for continuously varying cross-section beams.

The strain-nodal displacement relation of the sub-beam $m$ is directly obtained from Eq. (8)

$$\boldsymbol{\varepsilon}^{(m)} = \mathbf{B}^{(m)}\mathbf{U} \quad \text{with} \quad \boldsymbol{\varepsilon}^{(m)} = \begin{bmatrix} \varepsilon_{rr}^{(m)} & 2\varepsilon_{r\bar{y}}^{(m)} & 2\varepsilon_{r\bar{z}}^{(m)} \end{bmatrix}^T, \tag{11}$$

where $\boldsymbol{\varepsilon}^{(m)}$ and $\mathbf{B}^{(m)}$ are the strain vector and the strain-nodal displacement relation matrix, respectively, and the nodal displacement vector for the $q$-node beam finite element is

$$\mathbf{U} = \begin{bmatrix} u_1 & v_1 & w_1 & \theta_x^1 & \theta_y^1 & \theta_z^1 & \alpha_1 & \ldots & u_q & v_q & w_q & \theta_x^q & \theta_y^q & \theta_z^q & \alpha_q \end{bmatrix}^T. \tag{12}$$

Note that the number of DOFs used at a beam node is 7.

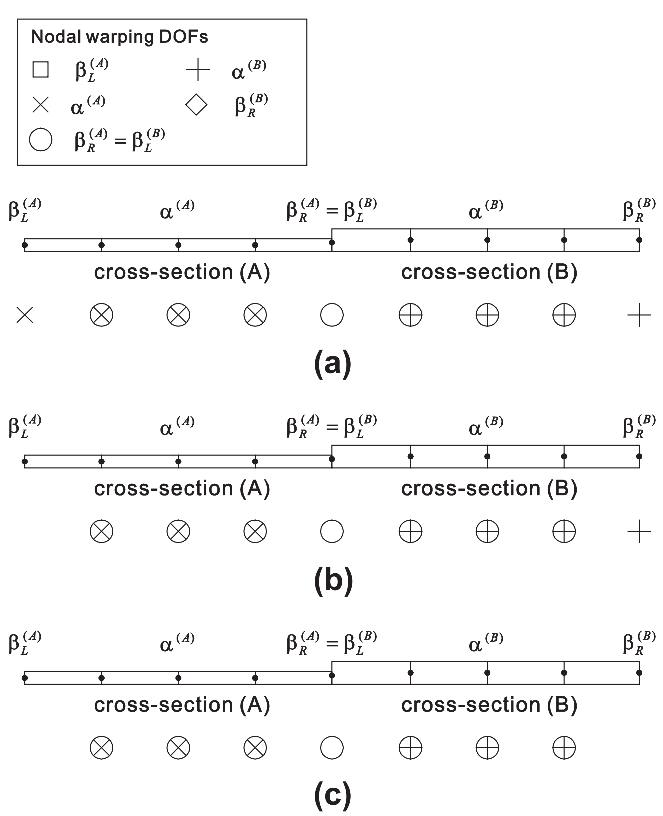


**Fig. 8.** Nodal warping DOFs used for (a) free–free, (b) constrained–free, (c) constrained–constrained warping problems.

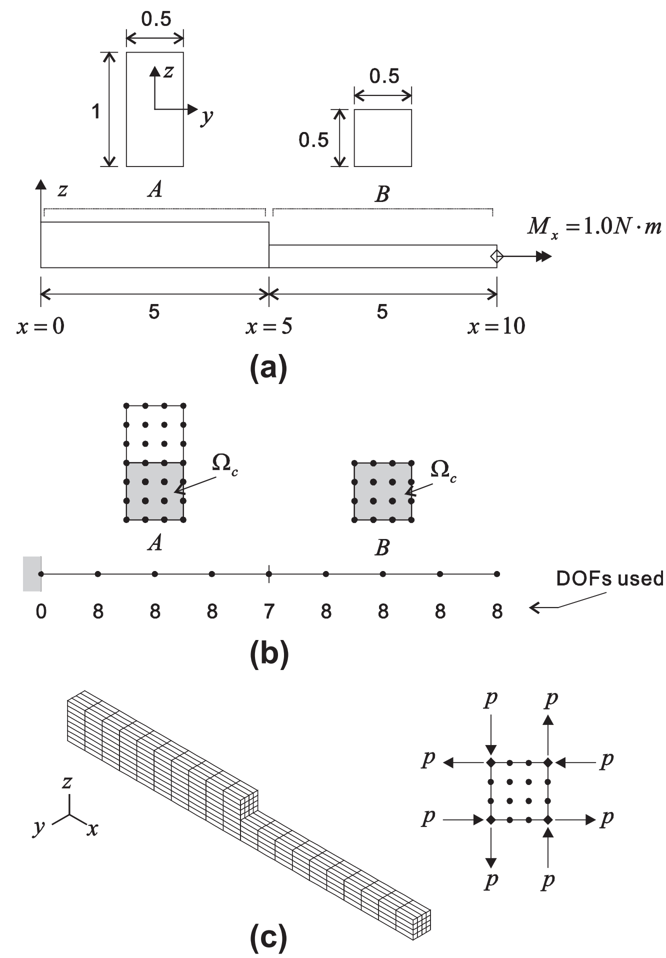


**Fig. 9.** Step varying rectangular cross-section problem. (a) Problem description (unit:m), (b) beam element model, cross-sectional mesh used and the number of each nodal DOFs used, (c) solid element model used.

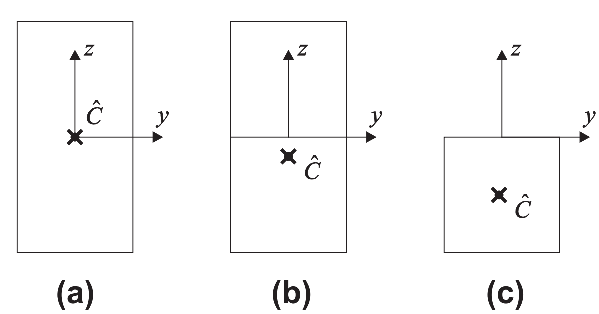


**Fig. 10.** Twisting centers in the step varying rectangular cross-section problem. (a) $(\lambda_y, \lambda_z) = (0, 0)$ for the free warping function of cross-section $A$, (b) $(\lambda_y, \lambda_z) = (0, -0.0833)$ for the interface warping function at $x = 5$ m, (c) $(\lambda_y, \lambda_z) = (0, -0.25)$ for the free warping function of cross-section $B$ .

Finally, the stiffness matrix of the continuum mechanics based beam finite element is numerically calculated by

$$\mathbf{K} = \sum_{m=1}^{n} \int_{V^{(m)}} \mathbf{B}^{(m)T}\mathbf{C}\mathbf{B}^{(m)} dV^{(m)} \tag{13}$$

in which $n$ is the number of sub-beams and, $V^{(m)}$ and $\mathbf{C}$ are respectively the volume of the sub-beam $m$ and the constitutive matrix for the beams [1]. To avoid transverse shear and membrane lockings,

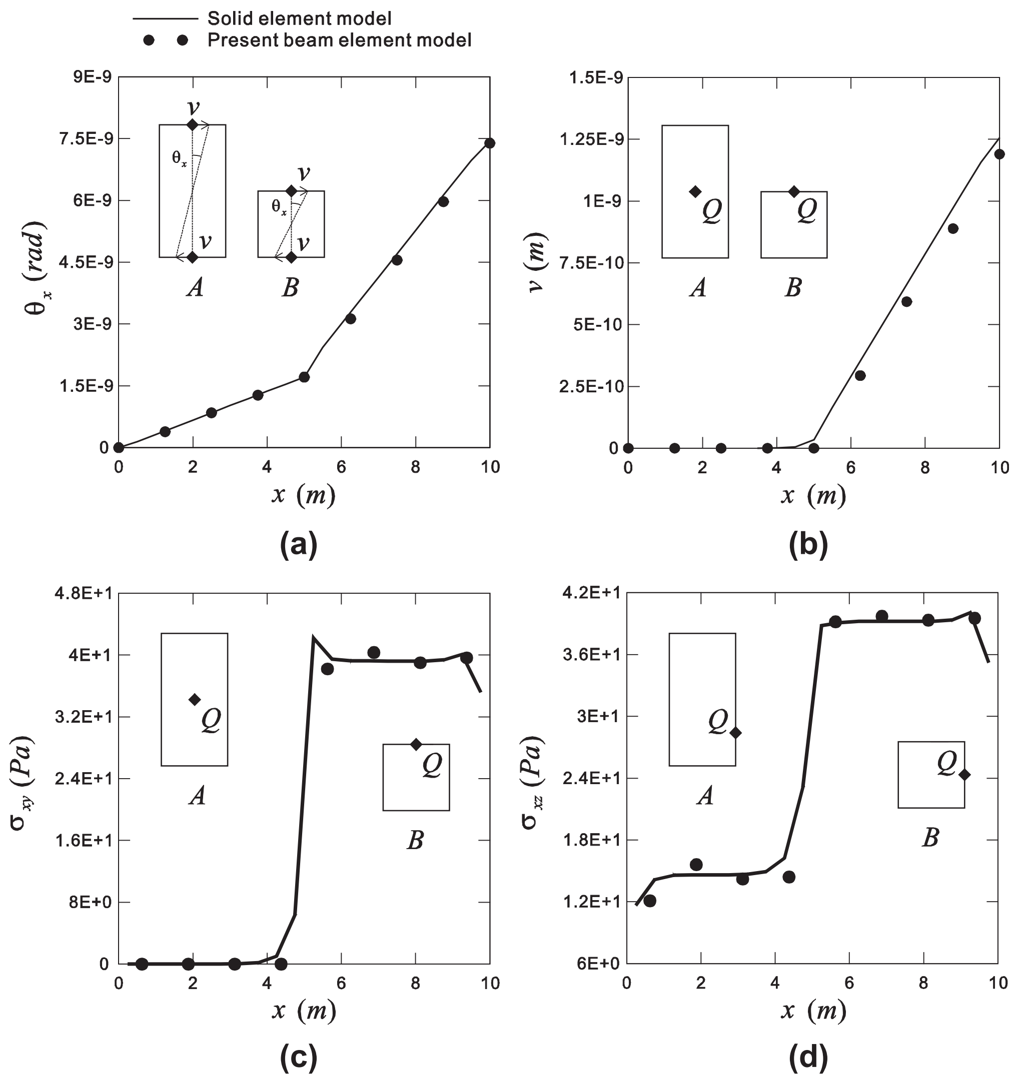


**Fig. 11.** Numerical results along the beam length in the step varying rectangular cross-section problem. (a) Angle of twist, (b) transverse displacement $v$ at Q, (c) shear stress $\sigma_{xy}$ at Q, (d) shear stress $\sigma_{xz}$ at Q.

the reduced integration technique or the MITC (Mixed Interpolation of Tensorial Components) method can be used [1,24,29]. Note that in this beam formulation the shear correction factor is not considered. Therefore, the equivalent shear correction factor used is 1.0 for all the numerical examples considered in this paper. However, it is not hard to employ the shear correction factor in this beam formulation. To do that, a simple decomposition of strains is necessary.

### 2.2. New warping displacement model

The variation in warping displacements is very complicated around discontinuous interfaces and the twisting center also varies along the beam length direction. Therefore, it is difficult to construct the warping displacement field by using only the free warping function obtained by St. Venant equation. The basic idea of this study is that the complicated warping displacement field $\mathbf{u}_w^{(m)}$ in Eq. (8) can be represented by a linear combination of the free warping function and the warping functions at the discontinuous interface. However, it is challenging to find the interface warping functions that satisfy the continuity of warping displacements. In particular, it is not easy to find the centers of the twist on the interface cross-sections. These were not found in previous studies.

We here define three basis warping functions: one free warping function ($f_k^{(m)}$) and two interface warping functions ($f_L^{(m)}$ and $f_R^{(m)}$) at both beam ends. A combination of these three basis warping functions with the corresponding three warping DOFs ($\alpha_k$, $\beta_L^k$ and $\beta_R^k$) constructs the continuous warping displacement fields for discontinuously varying cross-section beams

$$\mathbf{u}_w^{(m)}(r,s,t) = \sum_{k=1}^{q} h_k(r)\left[f_k^{(m)}(s,t)\alpha_k + f_L^{(m)}(s,t)\beta_L^k + f_R^{(m)}(s,t)\beta_R^k\right]\mathbf{V}_r^k. \quad (14)$$

Therefore, in general at most three warping DOFs are required at each beam node.

To demonstrate how to set up the warping DOFs, we consider a beam with a discontinuously varying cross-section, as shown in Fig. 4(a). The beam consists of two regions with different cross-sections. Beam regions A and B have cross-sections A and B, respectively. Each region is modeled by four beam finite elements, as shown in Fig. 4(b). In each beam region, all of the warping DOFs ($\alpha$, $\beta_L$ and $\beta_R$) are set to be continuous. Each beam region has interfaces at the left and right ends; that is, free and constrained ends are also considered as interfaces. At each interface, two warping DOFs except for the warping DOF corresponding to the interface are set to be zero, as shown in Fig. 4(b). At the interface of both

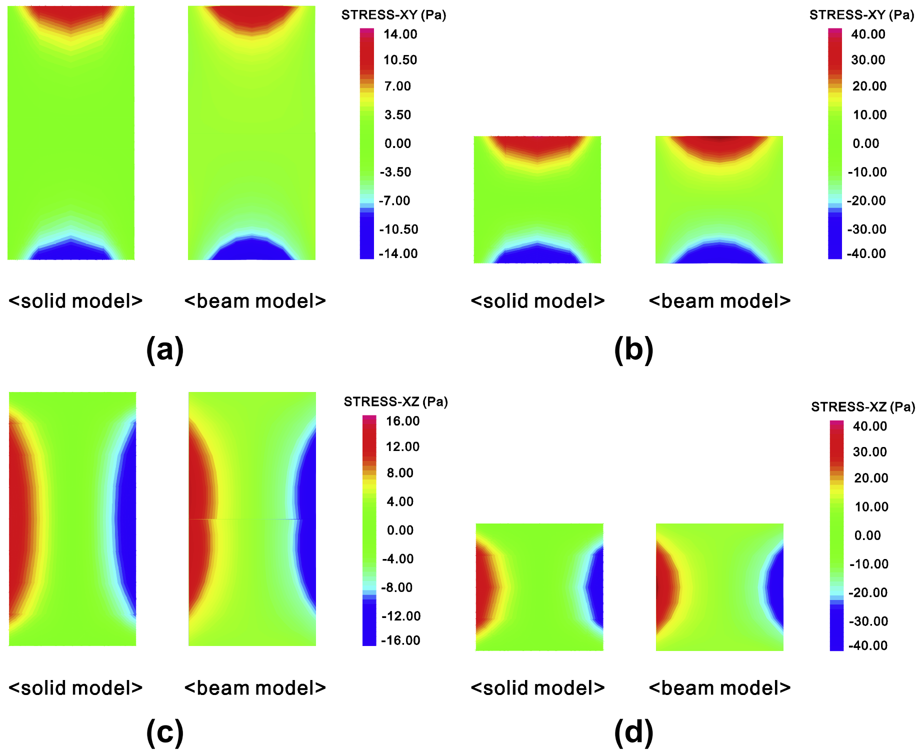


**Fig. 12.** Transverse shear stresses in the cross-section for the step varying rectangular cross-section problem. (a) $\sigma_{xy}$ at $x$ = 2.5 m, (b) $\sigma_{xy}$ at $x$ = 7.5 m, (c) $\sigma_{xz}$ at $x$ = 2.5 m, (d) $\sigma_{xz}$ at $x$ = 7.5 m.

beam regions, the interface warping DOFs $\beta_R^{(A)} = \beta_L^{(B)}$ and the other DOFs are set to be zero. Therefore, the interface DOFs make the warping displacements continuous at the interfaces. Fig. 4(c) shows the possible distributions of the warping DOFs along the beam length.

### 2.3. Free warping function

In our previous study [24], to calculate free warping functions, the following three-step calculation is required as in Ref. [30]: In the first step, St. Venant equation is solved for a certain arbitrary coordinate system. In the second step, the twisting center is calculated using the warping function obtained in the first step. In the third step, the final warping function is obtained by the coordinate transformation of the warping function obtained in the first step using the twisting center calculated in the second step.

Here we present a newly developed single-step method to simultaneously calculate the free warping function and the corresponding twisting center in arbitrary beam cross-sections.

Let us consider the cross-sectional domain $\Omega$ defined in the cross-sectional Cartesian coordinates $\bar{y}$ and $\bar{z}$ with the origin $C$, as shown in Fig. 5. The position of the origin $C$ can be arbitrarily chosen in the cross-section. The cross-sectional domain $\Omega$ is subjected to pure twisting kinematics about the twisting center $\widehat{C}$, where bending and transverse shearing are not involved. Then, the displacement fields are obtained as

$$u = kf, \quad v = -\hat{z}\theta_x \quad \text{and} \quad w = \hat{y}\theta_x \quad \text{in } \Omega, \tag{15}$$

where $k = \partial\theta_x/\partial x$, $f(\hat{y},\hat{z})$ is the warping function corresponding to the twisting center and $\hat{y}$ and $\hat{z}$ are the coordinates in the cross-sectional Cartesian coordinate system defined at the twisting center $\widehat{C}$ .

Note that in general the position of the twisting center $(\lambda_{\bar{y}}, \lambda_{\bar{z}})$ is unknown. After the warping function corresponding to the origin $C$ is obtained, the twisting center can be calculated, and then the correct warping function corresponding to the twisting center $\widehat{C}$ can be obtained through a transformation procedure, as in Refs. [24,30]. However, in the method proposed in this study, the warping function and the twisting center are obtained at the same time. This is a very important feature in obtaining the interface warping functions.

The displacement field in Eq. (15) results in the transverse shear stress fields

$$\tau_{x\hat{y}} = Gk\left(\frac{\partial f}{\partial \hat{y}} - \hat{z}\right) \quad \text{and} \quad \tau_{x\hat{z}} = Gk\left(\frac{\partial f}{\partial \hat{z}} + \hat{y}\right) \quad \text{in } \Omega \tag{16}$$

in which $G$ is the shear modulus. Note that other stresses are zero.

By applying Eq. (16) to the local equilibrium equations [24,30], the well-known St. Venant equations are obtained

$$G\left(\frac{\partial^2 f}{\partial \hat{y}^2} + \frac{\partial^2 f}{\partial \hat{z}^2}\right) = 0 \quad \text{in } \Omega, \quad n_{\hat{y}}\frac{\partial f}{\partial \hat{y}} + n_{\hat{z}}\frac{\partial f}{\partial \hat{z}} = n_{\hat{y}}\hat{z} - n_{\hat{z}}\hat{y} \quad \text{on } \Gamma, \tag{17}$$

where $(n_{\hat{y}}, n_{\hat{z}})$ is the vector normal to the cross-sectional boundary, see Fig. 5.

The variational formulation can be easily derived with the variation of the warping function $\delta f$,

$$\int_\Omega G\left(\frac{\partial f}{\partial \hat{y}}\frac{\partial \delta f}{\partial \hat{y}} + \frac{\partial f}{\partial \hat{z}}\frac{\partial \delta f}{\partial \hat{z}}\right) d\Omega = \int_\Gamma G(n_{\hat{y}}\hat{z} - n_{\hat{z}}\hat{y})\delta f \, d\Gamma. \tag{18}$$

Using the relation between the two cross-sectional Cartesian coordinate systems denoted as $(\bar{y},\bar{z})$ and $(\hat{y},\hat{z})$, $\hat{y} = \bar{y} - \lambda_{\bar{y}}$ and $\hat{z} = \bar{z} - \lambda_{\bar{z}}$, in Eq. (18), we obtain

$$G\int_\Omega \left(\frac{\partial f}{\partial \bar{y}}\frac{\partial \delta f}{\partial \bar{y}} + \frac{\partial f}{\partial \bar{z}}\frac{\partial \delta f}{\partial \bar{z}}\right) d\Omega + G\lambda_{\bar{z}} \int_\Gamma (n_{\bar{y}}\delta f) d\Gamma - G\lambda_{\bar{y}} \int_\Gamma (n_{\bar{z}}\delta f) d\Gamma = G\int_\Gamma (n_{\bar{y}}\bar{z} - n_{\bar{z}}\bar{y})\delta f \, d\Gamma. \tag{19}$$

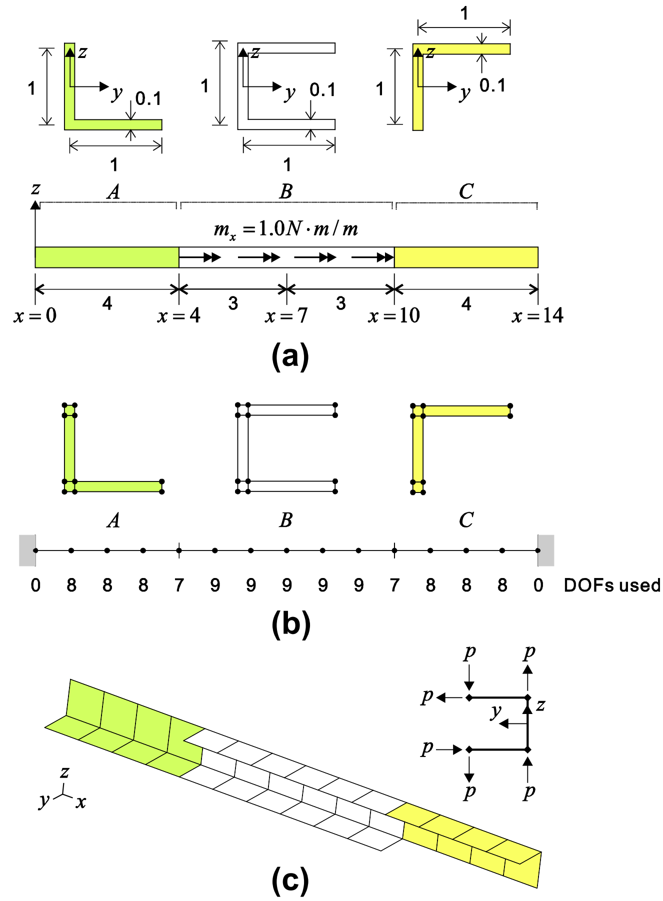


**Fig. 13.** Discontinuously varying thin-walled cross-section beam problem. (a) Problem description (unit:m), (b) beam element model, cross-sectional meshes used and the number of each nodal DOFs used, (c) shell element model used.

Since the pure twisting kinematics does not produce bending moments in the cross-section, the zero bending moment condition $M_{\bar{z}} = M_{\bar{y}} = 0$ gives

$$G\int_\Omega (\bar{y} - \bar{y}_{ave}) f \delta f \, d\Omega = 0 \quad \text{and} \quad G\int_\Omega (\bar{z} - \bar{z}_{ave}) f \delta f \, d\Omega = 0 \tag{20}$$

with the location of the cross-sectional centroid being

$$\bar{y}_{ave} = \frac{\int_\Omega \bar{y} d\Omega}{\int_\Omega d\Omega} \quad \text{and} \quad \bar{z}_{ave} = \frac{\int_\Omega \bar{z} d\Omega}{\int_\Omega d\Omega}. \tag{21}$$

In order to discretize the three equations in Eqs. (19) and (20), the warping function is interpolated as in Eq. (10). Applying the standard procedure of the finite element method, the matrix equations are obtained

$$\begin{bmatrix} G\mathbf{K} & G\mathbf{N}_{\bar{y}} & -G\mathbf{N}_{\bar{z}} \\ G\mathbf{H}_{\bar{y}} & \mathbf{0} & \mathbf{0} \\ G\mathbf{H}_{\bar{z}} & \mathbf{0} & \mathbf{0} \end{bmatrix} \begin{bmatrix} \mathbf{F} \\ \lambda_{\bar{z}} \\ \lambda_{\bar{y}} \end{bmatrix} = \begin{bmatrix} G\mathbf{B} \\ 0 \\ 0 \end{bmatrix} \quad \text{in } \Omega, \tag{22}$$

where $\mathbf{F}$ is the vector of the unknown nodal warping values, $\mathbf{K}$, $\mathbf{N}_{\bar{y}}$, and $\mathbf{N}_{\bar{z}}$ are the matrices obtained from the left-hand side of Eq. (19), $\mathbf{B}$ is the vector obtained from the right-hand side of Eq. (19), and $\mathbf{H}_{\bar{y}}$ and $\mathbf{H}_{\bar{z}}$ are the matrices obtained from Eq. (20). Solving Eq. (22), we can simultaneously calculate both the warping function and the corresponding twisting center.

### 2.4. Interface warping functions

The warping functions and the position of the corresponding twisting center at interfaces have not been studied before. In this section, we present a method to calculate the interface warping functions and the corresponding twisting center by solving a set of coupled equations.

Let us define the interface cross-sections, as shown in Fig. 6. The cross-sectional domains $\Omega^{(I)}$ and $\Omega^{(II)}$ have shear moduli $G_1$ and $G_2$, respectively. Eq. (22) can be rewritten for each cross-sectional domain

$$\begin{bmatrix} G_1\mathbf{K}^{(I)} & G_1\mathbf{N}_{\bar{y}}^{(I)} & -G_1\mathbf{N}_{\bar{z}}^{(I)} & \mathbf{L}^{(I)} \\ G_1\mathbf{H}_{\bar{y}}^{(I)} & \mathbf{0} & \mathbf{0} & \mathbf{0} \\ G_1\mathbf{H}_{\bar{z}}^{(I)} & \mathbf{0} & \mathbf{0} & \mathbf{0} \end{bmatrix} \begin{bmatrix} \mathbf{F}^{(I)} \\ \lambda_{\bar{z}} \\ \lambda_{\bar{y}} \\ \boldsymbol{\lambda} \end{bmatrix} = \begin{bmatrix} G_1\mathbf{B}^{(I)} \\ 0 \\ 0 \\ \mathbf{0} \end{bmatrix} \quad \text{for } \Omega^{(I)}, \tag{23}$$

$$\begin{bmatrix} G_2\mathbf{K}^{(II)} & G_2\mathbf{N}_{\bar{y}}^{(II)} & -G_2\mathbf{N}_{\bar{z}}^{(II)} & -\mathbf{L}^{(II)} \\ G_2\mathbf{H}_{\bar{y}}^{(II)} & \mathbf{0} & \mathbf{0} & \mathbf{0} \\ G_2\mathbf{H}_{\bar{z}}^{(II)} & \mathbf{0} & \mathbf{0} & \mathbf{0} \end{bmatrix} \begin{bmatrix} \mathbf{F}^{(II)} \\ \lambda_{\bar{z}} \\ \lambda_{\bar{y}} \\ \boldsymbol{\lambda} \end{bmatrix} = \begin{bmatrix} G_2\mathbf{B}^{(II)} \\ 0 \\ 0 \\ \mathbf{0} \end{bmatrix} \quad \text{for } \Omega^{(II)}, \tag{24}$$

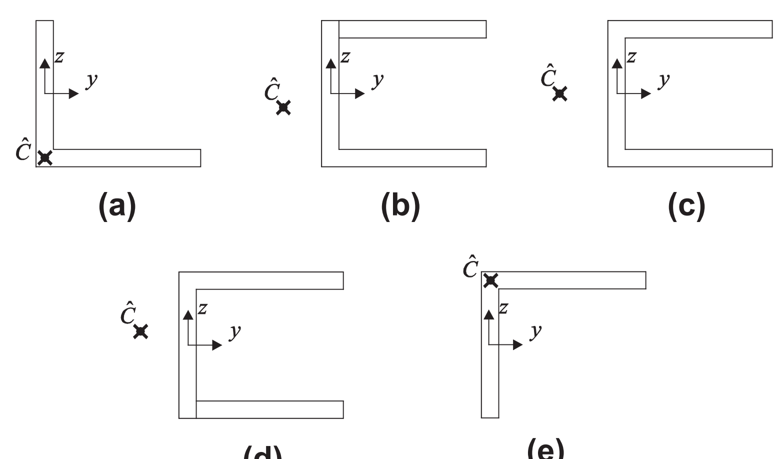


**Fig. 14.** Twisting centers in the discontinuously varying thin-walled cross-section beam problem. (a) (0.0037, −0.4952) for the free warping function of cross-section $A$, (b) (−0.3584, −0.1037) for the interface warping function at $x$ = 4 m, (c) (−0.4163, 0) for the free warping function of cross-section $B$, (d) (−0.3584, 0.1037) for the interface warping function at $x$ = 10 m, (e) (0.0037, 0.4952) for the free warping function of cross-section $C$ .

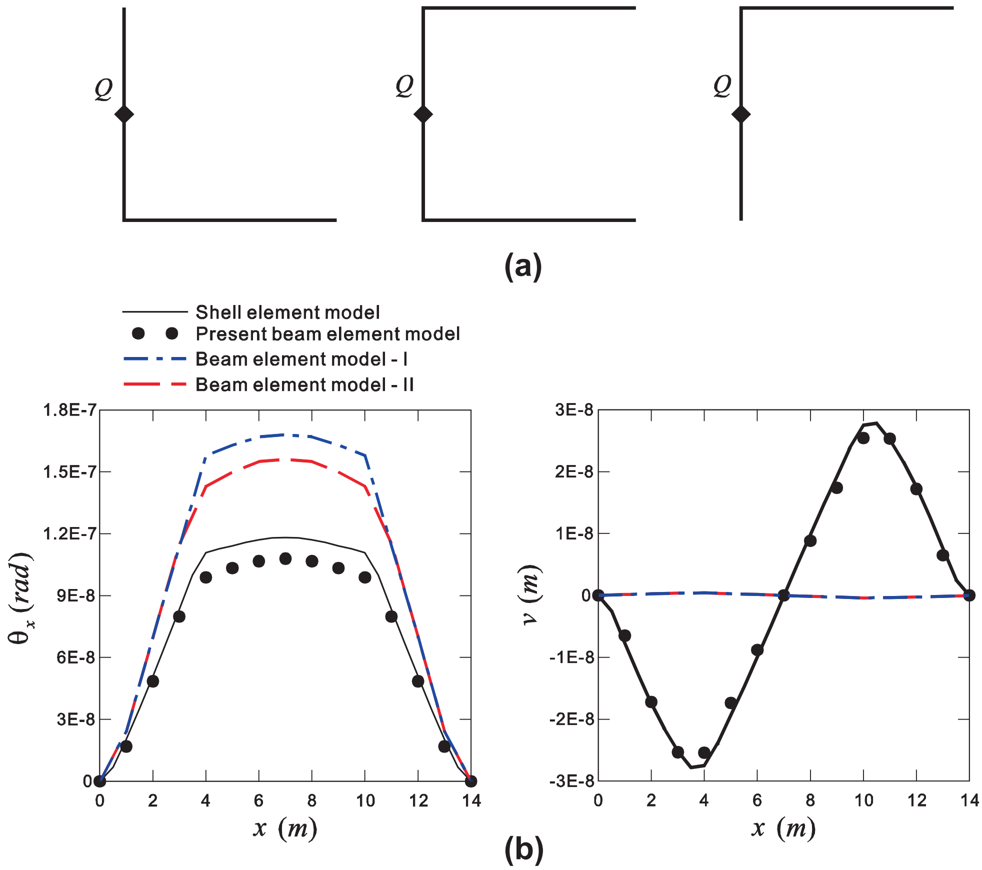


**Fig. 15.** Angle of twist and displacement $v$ along the beam length in the discontinuously varying thin-walled cross-section beam problem. (a) Sampling points $Q$ in the cross-sections, (b) angle of twist (left) and displacement $v$ (right).

where $\mathbf{L}^{(I)}$ and $\mathbf{L}^{(II)}$, and $\boldsymbol{\lambda}$ are Boolean matrices and the Lagrange multiplier vector, respectively, to enforce the constraint condition such that the warping values in both cross-sectional domains should be equal in the interconnected area $\Omega_C$

$$\begin{bmatrix} \mathbf{L}^{(I)T} & -\mathbf{L}^{(II)T} \end{bmatrix} \begin{bmatrix} \mathbf{F}^{(I)} \\ \mathbf{F}^{(II)} \end{bmatrix} = [\mathbf{0}] \quad \text{for } \Omega_C. \tag{25}$$

Eqs. (23)–(25) finally give a set of five coupled equations in a matrix form

$$\begin{bmatrix} G_1\mathbf{K}^{(I)} & \mathbf{0} & G_1\mathbf{N}_{\bar{y}}^{(I)} & -G_1\mathbf{N}_{\bar{z}}^{(I)} & \mathbf{L}^{(I)} \\ \mathbf{0} & G_2\mathbf{K}^{(II)} & G_2\mathbf{N}_{\bar{y}}^{(II)} & -G_2\mathbf{N}_{\bar{z}}^{(II)} & -\mathbf{L}^{(II)} \\ G_1\mathbf{H}_{\bar{y}}^{(I)} & G_2\mathbf{H}_{\bar{y}}^{(II)} & \mathbf{0} & \mathbf{0} & \mathbf{0} \\ G_1\mathbf{H}_{\bar{z}}^{(I)} & G_2\mathbf{H}_{\bar{z}}^{(II)} & \mathbf{0} & \mathbf{0} & \mathbf{0} \\ \mathbf{L}^{(I)T} & -\mathbf{L}^{(II)T} & \mathbf{0} & \mathbf{0} & \mathbf{0} \end{bmatrix} \begin{bmatrix} \mathbf{F}^{(I)} \\ \mathbf{F}^{(II)} \\ \lambda_{\bar{z}} \\ \lambda_{\bar{y}} \\ \boldsymbol{\lambda} \end{bmatrix} = \begin{bmatrix} G_1\mathbf{B}^{(I)} \\ G_2\mathbf{B}^{(II)} \\ 0 \\ 0 \\ \mathbf{0} \end{bmatrix} \tag{26}$$

in which the first and second equations are St. Venant equations corresponding to the two different cross-sectional domains, the third and fourth equations correspond to the zero bending moment conditions in Eq. (20), and the last equation is the constraint equation that enforces the continuity of warping in the interconnected cross-sectional area.

Solving Eq. (26), we can calculate the interface warping functions, which are used as basis warping functions in the warping displacement model for discontinuously varying cross-section beams.

It is essential to note three special cases for the interface warping functions, as shown in Fig. 7.

- *Free interface*: At the interface, no connected cross-section exists. This means that warping is free and the interface warping function thus becomes equal to the free warping function. Therefore, the corresponding interface warping DOF can be condensed out by setting it to zero.
- *Fully constrained interface*: The whole interface cross-section is connected to a rigid wall. Thus, warping is fully constrained and the corresponding interface warping function vanishes. Therefore, the corresponding interface DOF needs to be removed by setting it to zero.
- *Partially constrained interface*: A part of the interface is connected with a rigid wall. To solve this case, Eq. (26) should be modified. The cross-sectional domain $\Omega^{(II)}$ is assumed to be rigid. Using the condition $G_2 \to \infty$ in Eq. (26), we then obtain

$$\begin{bmatrix} \mathbf{K}^{(I)} & \mathbf{0} & \mathbf{N}_{\bar{y}}^{(I)} & -\mathbf{N}_{\bar{z}}^{(I)} & \mathbf{L}^{(I)} \\ \mathbf{0} & \mathbf{K}^{(II)} & \mathbf{N}_{\bar{y}}^{(II)} & -\mathbf{N}_{\bar{z}}^{(II)} & \mathbf{0} \\ \mathbf{0} & \mathbf{H}_{\bar{y}}^{(II)} & \mathbf{0} & \mathbf{0} & \mathbf{0} \\ \mathbf{0} & \mathbf{H}_{\bar{z}}^{(II)} & \mathbf{0} & \mathbf{0} & \mathbf{0} \\ \mathbf{L}^{(I)T} & \mathbf{0} & \mathbf{0} & \mathbf{0} & \mathbf{0} \end{bmatrix} \begin{bmatrix} \mathbf{F}^{(I)} \\ \mathbf{F}^{(II)} \\ \lambda_{\bar{z}} \\ \lambda_{\bar{y}} \\ \boldsymbol{\lambda} \end{bmatrix} = \begin{bmatrix} \mathbf{B}^{(I)} \\ \mathbf{B}^{(II)} \\ 0 \\ 0 \\ \mathbf{0} \end{bmatrix}. \tag{27}$$

Fig. 8 shows the DOFs used for the free-free, constrained-free, and constrained-constrained warping conditions. Finally, we note that when beams have a continuously varying cross-section, as shown in Fig. 1(a), two interface warping functions ($f_L^{(m)}$ and $f_R^{(m)}$) become equal to the free warping function ($f_k^{(m)}$). Therefore, the interface warping functions can be condensed out, and only the free warping function and the corresponding DOF are necessary in the beam element formulation.

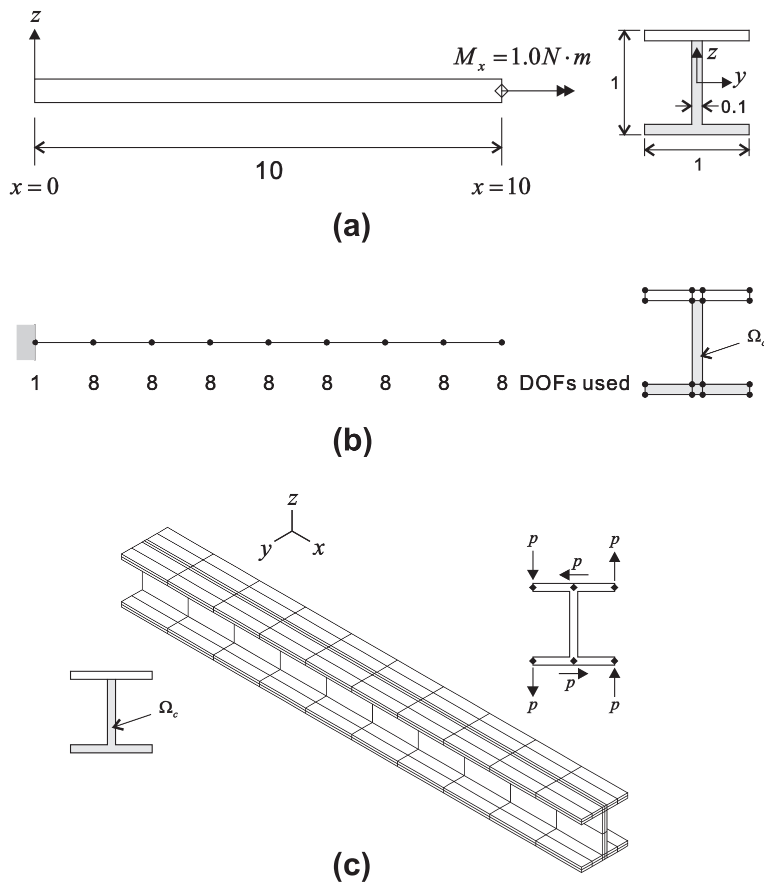


**Fig. 16.** Partially constrained warping problem. (a) Problem description (unit:m), (b) beam element model, cross-sectional mesh used, constrained warping area (shaded area) and the numbers of the nodal DOFs used, (c) solid element model used.

## 3. Numerical results

To verify the performance of the warping displacement model proposed in this study, we numerically solve three beam problems: a step varying rectangular cross-section problem, a discontinuously varying thin-walled cross-section problem, a partially constrained warping problem, and a curved beam problem with a discontinuously varying cross-section. The results are compared with reference solutions obtained by using refined solid and shell element models. In addition, the solutions of the beam element model with the warping displacement model in Eq. (9) are compared. Note that two-node linear beam finite elements are used for all of the beam models and that the well-known reduced integration is employed in order to avoid shear locking [1,24,29]. A Young's modulus $E = 2.0 \times 10^{11}$ N/m$^2$ and a Poisson's ratio $\nu = 0$ are used for all of the beam problems considered in this section.[1]

### 3.1. Step varying rectangular cross-section problem

We consider a step varying rectangular cross-section problem with two beam regions corresponding to two different cross-sections, $A$ and $B$, as shown in Fig. 9(a). All of the displacements including warping are constrained at $x = 0$ m and a torsional moment $M_x = 1.0$ Nm is applied at $x = 10$ m. The rectangular cross-section is discontinuous at $x = 5$ m. The beam problem is modeled by the proposed beam element, as shown in Fig. 9(b). The cross-sections $A$ and $B$ are discretized by two and one 16-node

[1] In order to avoid difficulties in specifying boundary conditions in equivalent shell and solid finite element models, zero Poisson's ratio is used.

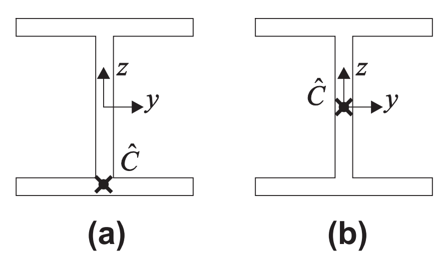


**Fig. 17.** Twisting centers in the partially constrained warping problem. (a) $(\lambda_y, \lambda_z) = (0, -0.4369)$ for the interface warping function at $x = 0$ m, (b) $(\lambda_y, \lambda_z) = (0, 0)$ for the free warping function.

cubic cross-sectional elements, respectively, and have an interconnected area $\Omega_c$ at $x = 5$ m.

The beam region with cross-section $A$ is modeled by four beam elements that have eight nodal DOFs $\begin{bmatrix} u & v & w & \theta_x & \theta_y & \theta_z & \alpha^{(A)} & \beta_R^{(A)} \end{bmatrix}^T$. The interface warping DOF $\beta_L^{(A)}$ is removed by setting $\beta_L^{(A)} = 0$ because beam region $A$ has a fully constrained interface at its left end ($x = 0$ m). The beam region with cross-section $B$ is modeled by four beam elements with eight nodal DOFs $\begin{bmatrix} u & v & w & \theta_x & \theta_y & \theta_z & \alpha^{(B)} & \beta_L^{(B)} \end{bmatrix}^T$. Setting $\beta_R^{(B)} = 0$, the interface warping DOF $\beta_R^{(B)}$ is condensed out because beam region $B$ has a free interface at its right end. At $x = 5$ m, the interface warping function is shared through the continuity of interconnected DOFs $(\beta_R^{(A)} = \beta_L^{(B)})$ and $\alpha^{(A)} = \alpha^{(B)} = 0$ at the interface node. The boundary condition $u = v = w = \theta_x = \theta_y = \theta_z = \alpha^{(A)} = \beta_R^{(A)} = 0$ is

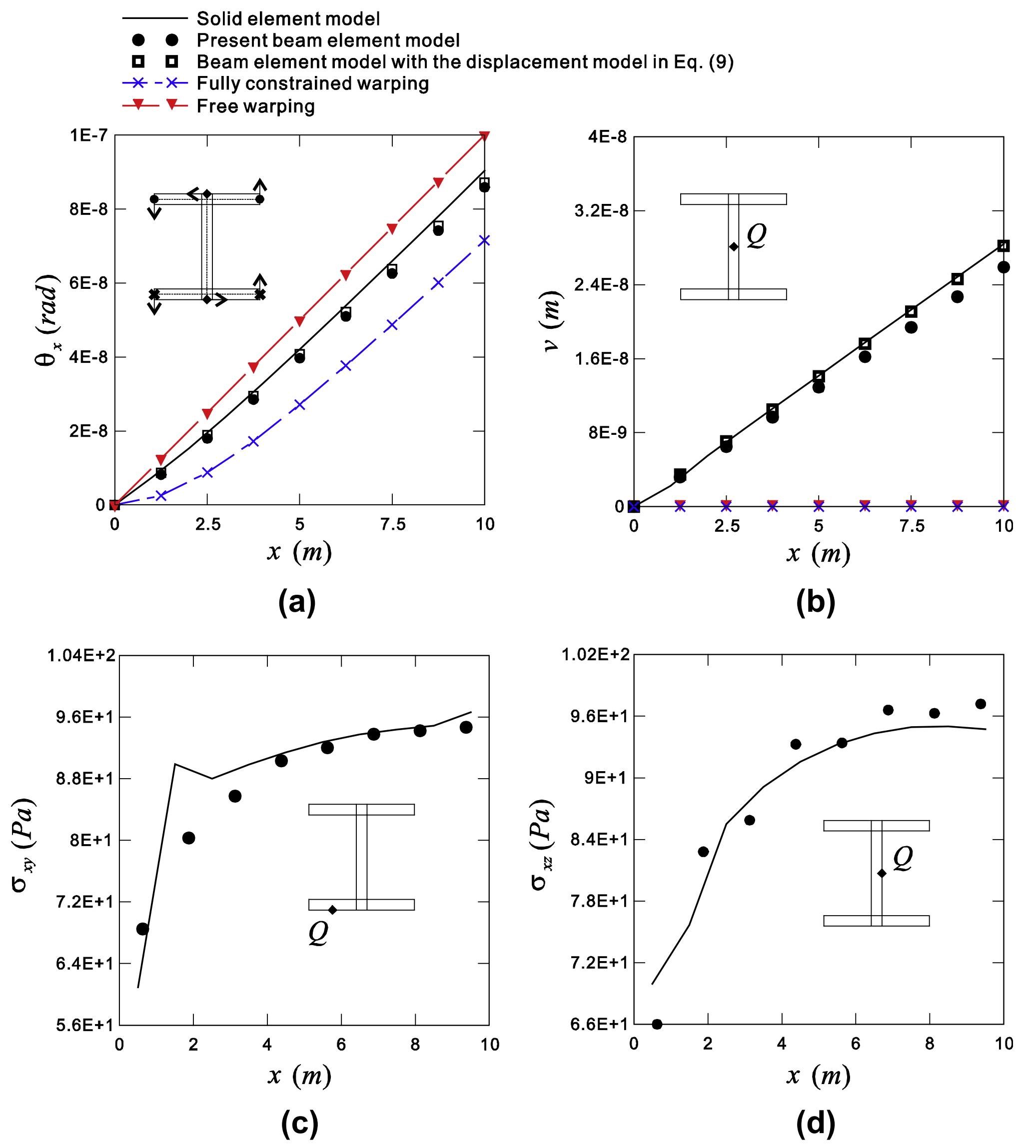


**Fig. 18.** Numerical results of the partially constrained warping problem. (a) Angle of twist, (b) displacement $v$ at Q, (c) Shear stress $\sigma_{xy}$ at Q, (d) shear stress $\sigma_{xz}$ at Q.

applied at $x = 0$ m. The numbers of the nodal DOFs used are presented in Fig. 9(b).

To calculate the reference solutions, 27-node quadratic solid finite elements are used, as shown in Fig. 9(c). In the solid element model, point loads ($p = 0.5$ N) are applied to obtain the equivalent torsional moment $M_x = 1.0$ N m at $x = 10$ m and all DOFs are fixed at $x = 0$ m.

Fig. 10 shows the positions of the twisting center for the free warping function of cross-sections $A$ and $B$, and for the interface warping function at $x = 5$ m. The variation of the twisting center along the beam length is automatically considered through the warping displacement field in Eq. (11).

Fig. 11 presents the numerical results along the beam length: showing the distribution of the angle of twist, displacement $v$, and transverse shear stresses $\sigma_{xy}$ and $\sigma_{xz}$ at point $Q$. Fig. 12 shows the distributions of transverse shear stresses $\sigma_{xy}$ and $\sigma_{xz}$ on the cross-sectional planes at $x = 2.5$ m and $x = 7.5$ m. The numerical results demonstrate the excellent predictive capability of the warping displacement model proposed in this study. Note that the numbers of DOFs used are 63 and 4680 in the beam and solid element models, respectively.

### 3.2. Discontinuously varying thin-walled cross-section problem

Let us consider a beam that consists of three beam regions corresponding to three different thin-walled cross-sections, $A$, $B$ and $C$, see Fig. 13(a). All displacements including warping are constrained at both ends ($x = 0$ m and $x = 14$ m) and a distributed torsional moment $M_x = 1.0$ Nm/m is applied at beam region $B$. The cross-section are discontinuous at $x = 4$ m and $x = 10$ m. The physical problem is modeled by the proposed beam element model, as shown in Fig. 13(b). The cross-sections $A$, $B$ and $C$ are discretized by four-node linear cross-sectional elements, and the cross-sectional meshes are interconnected at $x = 4$ m and $x = 10$ m.

Beam region $A$ is modeled by four beam elements that have eight nodal DOFs $\begin{bmatrix} u & v & w & \theta_x & \theta_y & \theta_z & \alpha^{(A)} & \beta_R^{(A)} \end{bmatrix}^T$. The interface warping DOF $\beta_L^{(A)}$ is set to zero because the warping is fully constrained at $x = 0$ m. Beam region $B$ is modeled by six beam elements with nine nodal DOFs $\begin{bmatrix} u & v & w & \theta_x & \theta_y & \theta_z & \alpha^{(B)} & \beta_L^{(B)} & \beta_R^{(B)} \end{bmatrix}^T$. Beam region $C$ is modeled by four beam elements with eight nodal DOFs $\begin{bmatrix} u & v & w & \theta_x & \theta_y & \theta_z & \alpha^{(C)} & \beta_L^{(C)} \end{bmatrix}^T$. The interface warping

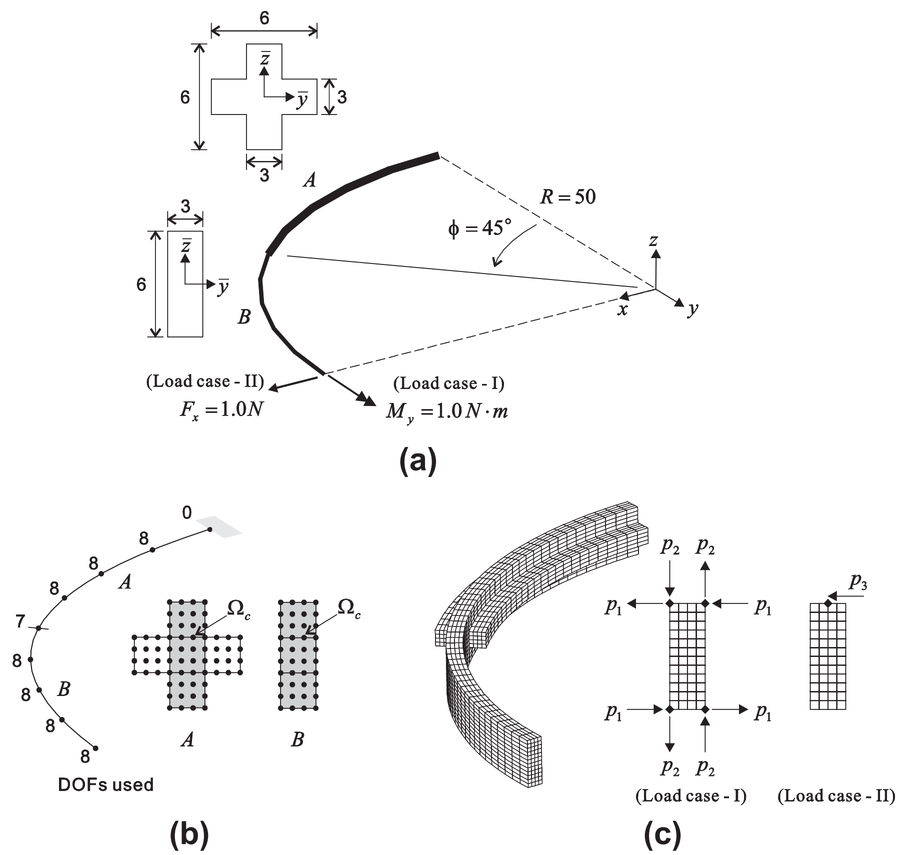

**Fig. 19.** Curved beam problem. (a) Problem description (unit:m), (b) beam element model, cross-sectional meshes used and the numbers of nodal DOFs used, (c) solid element model used ($p_1$ = 0.041667 N, $p_2$ = 0.125 N, $p_3$ = 1.0 N).

DOF $\beta_R^{(C)}$ is set to zero because the warping is fully constrained at $x$ = 14 m. The interface warping functions are shared at $x$ = 4 m and $x$ = 10 m for the continuity of interconnected DOFs ($\beta_R^{(A)} = \beta_L^{(B)}$ and $\beta_R^{(B)} = \beta_L^{(C)}$) and $\alpha^{(A)} = \alpha^{(B)} = \alpha^{(C)} = 0$ at the interfaces. The boundary conditions $u = v = w = \theta_x = \theta_y = \theta_z = \alpha^{(A)} = \beta_R^{(A)} = 0$ and $u = v = w = \theta_x = \theta_y = \theta_z = \alpha^{(C)} = \beta_L^{(C)} = 0$ are applied at $x$ = 0 m and $x$ = 14 m, respectively. The numbers of the nodal DOFs used are presented in Fig. 13(b).

To obtain the reference solutions, MITC9 shell finite elements are used in the shell element model shown in Fig. 13(c) [31–34]. Point loads ($p$ = 1/3 N/m) are distributed along beam region $B$, which produces the equivalent distributed torsional moment $m_x$ = 1.0 Nm/m. Therefore, the torsion is non-uniform along beam region $B$.

Fig. 14 shows the positions of the twisting centers for the free warping functions in cross-sections $A$, $B$, and $C$ and for the interface warping functions at $x$ = 4 m and $x$ = 10 m. Fig. 15(b) presents the distributions of the angle of twist and displacement $v$ along the beam length corresponding to point $Q$ in Fig. 15(a). The present beam element model (total 113 DOFs) with the proposed warping displacement model gives an angle of twist very close to that of the reference shell element model (total 805 DOFs). The figure shows that the transverse displacement of the present beam element model is also correctly calculated, because, in the beam element formulation, warping is fully coupled with stretching, shearing, and bending.

In Fig. 15(b), we also present the results when the continuity of warping is not properly considered. In the beam element models – I and II, only one warping function (the free warping function) and the corresponding warping DOF are employed. In the beam element model-I, the warping displacement field is not continuous at the interface cross-sections. Therefore, two independent warping DOFs are used at the interface cross-sections. In the beam element model-II, the warping DOFs are shared at the interface cross-section. Note that these two models are only available in most commercial FE software to consider the continuity of warping. Fig. 15(b) demonstrates the importance of the proper modeling of warping displacements. In particular, the displacement $v$ could be incorrectly approximated when the modeling of warping displacements is not proper.

### 3.3. Partially constrained warping problem

We consider a wide flange beam problem with a partially constrained warping condition as shown in Fig. 16(a). At $x$ = 0 m, all displacements including warping are constrained only at the shaded area $\Omega_c$ in Fig. 16(a) and (b), and torsional moment $M_x$ = 1.0 N m is applied at $x$ = 10 m.

The beam finite element model is shown in Fig. 16(b). The wide flange cross-section is discretized by seven four-node linear cross-sectional elements, and has a partially constrained interface at $x$ = 0 m. The beam is modeled by eight beam elements with eight nodal DOFs $[u \quad v \quad w \quad \theta_x \quad \theta_y \quad \theta_z \quad \alpha \quad \beta_L]^T$. The interface warping DOF $\beta_R$ is set to zero owing to the free interface at $x$ = 10 m. The boundary condition $u = v = w = \theta_x = \theta_y = \theta_z = \alpha = 0$ is applied at $x$ = 0 m. The numbers of the nodal DOFs used are presented in Fig. 16(b).

27-Node solid finite elements are used to obtain reference solutions, see Fig. 16(c). Point loads ($p$ = 1/3 N) are applied in the solid element model for the equivalent torsional moment $M_x$ = 1.0 Nm, and all DOFs corresponding to the shaded area $\Omega_c$ are fixed at $x$ = 0 m.

Fig. 17 shows the positions of the twisting centers for the interface warping function at $x$ = 0 m and the free warping function of the wide flange cross-section. Fig. 18 presents the angle of twist,

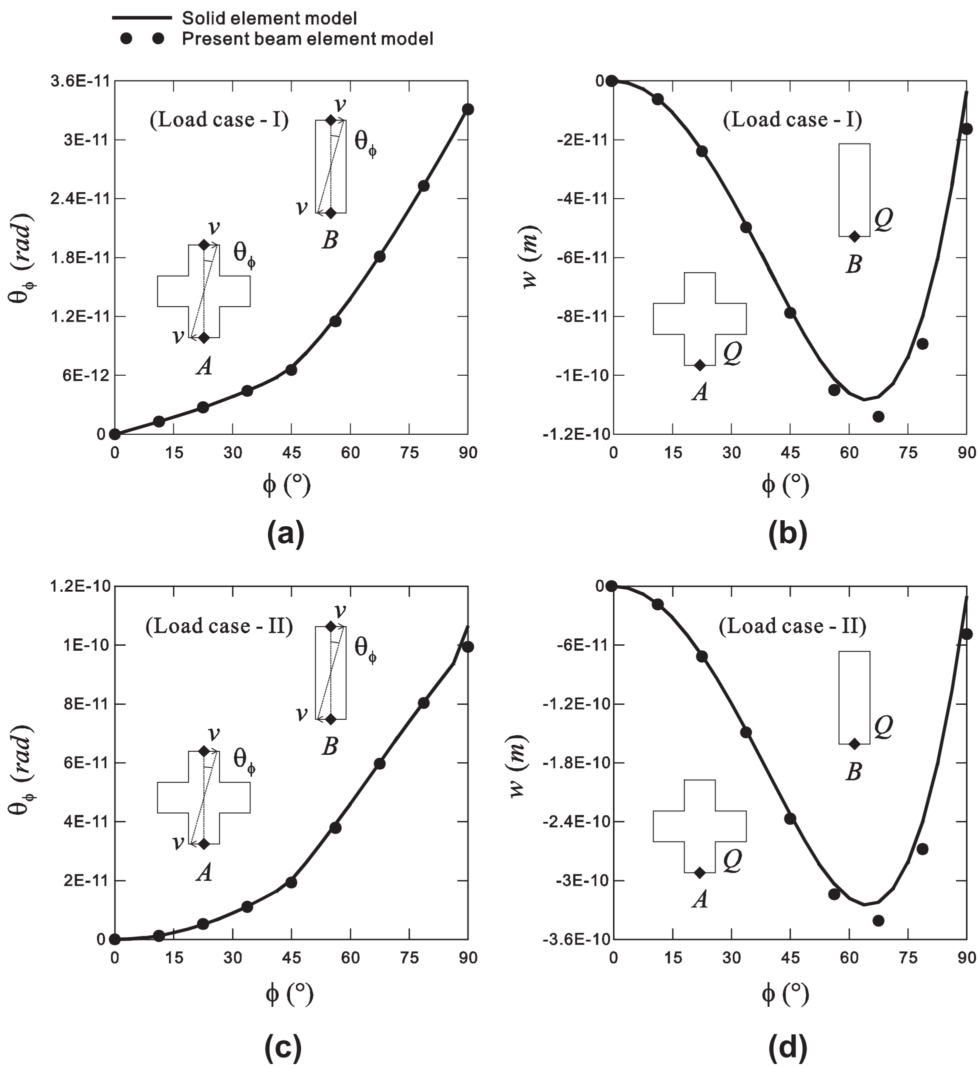


**Fig. 20.** Numerical results of the curved beam problem along the beam length. (a) Angle of twist $\theta_\phi$ for the load case – I, (b) displacement $w$ for the load case – I, (c) angle of twist $\theta_\phi$ for the load case – II, (d) displacement $w$ for the load case – II.

displacement $v$, and transverse shear stresses $\sigma_{xy}$ and $\sigma_{xz}$ at point $Q$ along the beam length. The results of the beam element model (total 65 DOFs) with the proposed warping displacement model are compared with those the reference solid element model (total 8,880 DOFs) and the beam element model (total 174 DOFs) with the warping displacement model in Eq. (9), which uses 16 warping DOFs at each beam node in this beam problem.

The results of the two beam element models show good agreement with the reference solution calculated by the solid element model. The numbers of DOFs used show the effectiveness of the present beam model. We show the results for free and fully constrained warping cases. As expected, the angle of twist of the partially constrained case exists between those of both cases. While the displacement $v$ of the free and fully constrained warping cases is zero, the partially constrained warping case results in non-zero displacement $v$. This indicates that the twisting centers are properly considered in the present warping displacement model.

### 3.4. Curved beam problem with a discontinuously varying cross-section

We consider a curved beam problem with discontinuously varying cross-sections: from the cross-shaped cross-section $A$ to the rectangular cross-section $B$ as shown in Fig. 19(a).

The cross-section discontinuously varies from $A$ to $B$ at $\phi = 45°$. All displacements including warping are constrained at $\phi = 0°$ and two load cases are considered:

(Load case – I) A torsional moment $M_y = 1.0$ Nm is applied at $\phi = 90°$.

(Load case – II) An eccentric shear force $F_x = 1.0$ N is applied at $\phi = 90°$.

As shown in Fig. 19(b), the cross-sections $A$ and $B$ are discretized by 16-node cubic cross-sectional elements with an interconnected domain $\Omega_c$ at $\phi = 45°$. Beam region $A$ is modeled by four beam elements with eight nodal DOFs $\begin{bmatrix} u & v & w & \theta_x & \theta_y & \theta_z & \alpha^{(A)} & \beta_R^{(A)} \end{bmatrix}^T$. The interface warping DOF $\beta_L^{(A)}$ is set to zero due to the fully constrained interface at $\phi = 0°$. Beam region $B$ is modeled by four beam elements with eight nodal DOFs $\begin{bmatrix} u & v & w & \theta_x & \theta_y & \theta_z & \alpha^{(B)} & \beta_L^{(B)} \end{bmatrix}^T$. The interface warping DOF $\beta_R^{(B)}$ is set to zero due to the free interface at $\phi = 90°$. The continuity of the warping displacement is ensured by the condition $\beta_R^{(A)} = \beta_L^{(B)}$ at $\phi = 45°$. The boundary condition $u = v = w = \theta_x = \theta_y = \theta_z = \alpha^{(A)} = \beta_R^{(A)} = 0$ is used at $\phi = 0°$. The numbers of the nodal DOFs used are presented in Fig. 19(b).

To obtain the reference solutions, 27-node solid elements are used, as shown in Fig. 19(c). In the solid element model, point loads ($p_1$ = 0.041667 N and $p_2$ = 0.125 N) are applied for load case – I and a point load ($p_3$ = 1.0 N) is applied for load case – II at $\phi$ = 90°. All DOFs are fixed at $\phi$ = 0°.

Fig. 20 shows the angle of twist and displacement $v$ at point $Q$ along the beam length. The results of the beam element model (total 69 DOFs) with the proposed warping displacement model show good agreement with those of the reference solid element model (total 85,536 DOFs). It is very difficult to calculate the response of this curved beam problem accurately without properly considering the flexure–torsion coupling effect.

## 4. Conclusions

In this paper, we proposed a new modeling method to construct continuous warping displacement fields for beams with discontinuously varying arbitrary cross-sections. The warping displacement is represented by a combination of three basis warping functions (one free warping function and two interface warping functions) accompanying the corresponding three warping DOFs that are interpolated along the beam length. We also introduced a new numerical method that calculates the free warping functions and the twisting centers simultaneously. Using this method and Lagrange multipliers, a set of coupled equations was formulated to obtain interface warping functions.

All of the methods proposed in this study can be generally used for beams with arbitrary cross-sections including solid and thin and thick-walled cross-sections. We presented three numerical examples to show the feasibility and effectiveness of the proposed warping displacement model. The proposed modeling method to construct the warping displacement fields can significantly reduce the required number of DOFs.

Although the method proposed here was demonstrated the basis of the continuum mechanics based beam finite elements, the concept can be easily adopted to other types of beam finite elements allowing warping displacements. A direct extension of the proposed method for nonlinear analyses is a worthwhile topic for future studies, as in Refs. [35–37]. Further, it is important to note that in this study we considered only the continuity of primary torsional warping displacements in discontinuously varying cross-section beams. However, the same method can be employed for secondary torsional warping and shear warping displacements.

## Acknowledgments

This research was supported by Basic Science Research Program through the National Research Foundation of Korea (NRF) funded by the Ministry of Science, ICT and Future Planning (No. 2011-0014387).

## References

[1] Bathe KJ. Finite element procedures. New York: Prentice Hall; 1996.
[2] Timoshenko SP, Goodier JN. Theory of elasticity. McGraw Hill; 1970.
[3] Vlasov VZ. Thin-walled elastic beams. Jerusalem: Israel Program for Scientific Translations; 1961.
[4] Krahula JL, Lauterbach GF. A finite element solution for Saint-Venant torsion. AIAA J 1969;7:2200–3.
[5] Kawai T. The application of finite element methods to ship structures. Comput Struct 1973;3:1175–94.
[6] Noor AK, Andersen CM. Mixed isoparametric elements for Saint-Venant torsion. Comput Methods Appl Mech Eng 1975;6:195–218.
[7] Dvorkin EN, Celentano D, Cuitino A, Gioia G. A Vlasov beam element. Comput Struct 1989;33:187–96.
[8] Gunnlaugsson GA, Pedersen PT. A finite element formulation for beams with thin walled cross-sections. Comput Struct 1982;15:691–9.
[9] Laudiero F, Savoia M. Shear strain effects in flexure and torsion of thin-walled beams with open or closed cross-section. Thin-Walled Struct 1990;10:87–119.
[10] Shakourzadeh H, Guo YQ, Batoz JL. A torsion bending element for thin-walled beams with open and closed cross sections. Comput Struct 1995;55:1045–54.
[11] Park SW, Fujii D, Fujitani Y. A finite element analysis of discontinuous thin-walled beams considering nonuniform shear warping deformation. Comput Struct 1997;65:17–27.
[12] Roberts TM, Al-Ubaidi H. Influence of shear deformation on restrained torsional warping of pultruded FRP bars of open cross section. Thin-Walled Struct 2001;39:395–414.
[13] Fatmi RE. Non-uniform warping including the effects of torsion and shear forces. Part I: A general beam theory. Int J Solids Strcut 2007;44:5912–29.
[14] Sapountzakis EJ, Mokos VG. 3-D beam element of composite cross section including warping and shear deformation effects. Comput Struct 2007;85:102–16.
[15] Ferradi MK, Cespedes X, Arquier M. A higher order beam finite element with warping eigenmodes. Eng Strut 2013;46:748–62.
[16] Genoese A, Genoese A, Bilotta A, Garcea G. A mixed beam model with non-uniform warpings derived from the Saint Venant rod. Comput Struct 2013;121:87–98.
[17] Mokos VG, Sapountzakis EJ. Secondary torsional moment deformation effect by BEM. Int J Mech Sci 2011;53:897–909.
[18] Bathe KJ, Chaudhary A. On the displacement formulation of torsion of shafts with rectangular cross-section. Int J Numer Methods Eng 1982;18:1565–8.
[19] Back SY, Will KM. A shear-flexible element with warping for thin-walled open beams. Int J Numer Methods Eng 1998;43:1173–91.
[20] Minghini F, Tullini N, Laudiero F. Locking-free finite elements for shear deformable orthotropic thin-walled beams. Int J Numer Methods Eng 2007;72:808–34.
[21] Carrera E, Guunta G, Nali P, Petrolo M. Refined beam elements with arbitrary cross-section geometries. Comput Struct 2010;88:283–93.
[22] Gonçalves R, Ritto-Corrêa M, Camotim D. A large displacement and finite rotation thin-walled beam formulation including cross-section deformation. Comput Methods Appl Mech Eng 2010;199:1627–43.
[23] Wackerfuß J, Gruttmann F. A nonlinear Hu–Washizu variational formulation and related finite element implementation for spatial beams with arbitrary moderate thick cross-sections. Comput Methods Appl Mech Eng 2011;200:1671–90.
[24] Yoon K, Lee YG, Lee PS. A continuum mechanics based beam finite element with warping displacements and its modeling capabilities. Struct Eng Mech 2012;43:411–37.
[25] Lee SW, Kim YH. A new approach to the finite element modelling of beams with warping effect. Int J Numer Methods Eng 1987;24:2327–41.
[26] Stemple AD, Lee SW. A finite element model for composite beams undergoing large deflection with arbitrary cross-sectional warping. Int J Numer Methods Eng 1989;28:2143–60.
[27] Prokić A. Thin-walled beams with open and closed cross-sections. Comput Struct 1993;47:1065–70.
[28] Živkovic M, Kojić M, Slavković R, Grujović N. A general beam finite element with deformable cross-section. Comput Methods Appl Mech Eng 2001;190:2651–80.
[29] Lee PS, Noh HC, Choi CK. Geometry-dependent MITC method for a 2-node iso-beam element. Struct Eng Mech 2008;29:203–21.
[30] Gruttmann F, Sauer R, Wagner W. Shear stresses in prismatic beams with arbitrary cross-sections. Int J Numer Methods Eng 1999;45:865–89.
[31] Bathe KJ, Lee PS, Hiller JF. Towards improving the MITC9 shell element. Comput Struct 2003;81:477–89.
[32] Chapelle D, Bathe KJ. The finite element analysis of shells-fundamentals. Berlin: Springer-Verlag; 2011.
[33] Lee PS, Bathe KJ. Insight into finite element shell discretizations by use of the basic shell mathematical model. Comput Struct 2005;83:69–90.
[34] Lee YG, Yoon K, Lee PS. Improving the MITC3 shell finite element by using the Hellinger–Reissner principle. Comput Struct 2012;110–111:93–106.
[35] Lee PS, McClure G. A general 3D L-section beam finite element for elastoplastic large deformation analysis. Comput Struct 2006;84:215–29.
[36] Lee PS, McClure G. Elastoplastic large deformation analysis of a lattice steel tower structure and comparison with full-scale tests. J Constr Steel Res 2007;63:709–17.
[37] Lee PS, Noh HC. Inelastic buckling behavior of steel members under reversed cyclic loading. Eng Struct 2010;32:2579–95.